Transp Porous Med (2012) 93:51–61
DOI 10.1007/s11242-012-9943-x

AC Diffusion: Transport in Porous Networks Subjected to Zero-Time-Average Advective Flow

J. J. Claria · G. H. Goldsztein · J. C. Santamarina

Received: 27 August 2010 / Accepted: 14 January 2012 / Published online: 3 February 2012

Abstract Diffusion is a slow transport mechanism and advective transport tends to dominate in large-size systems. An alternative transport mechanism is explored herein, whereby zero time-average cyclic fluid flow is compounded with pore-scale mixing to render effective transport. Two one-dimensional cyclic flow cases are analyzed: a rigid porous network with two open boundaries subjected to cyclic flow through, and a compressible porous network with only one open boundary subjected to cyclic compression. The corresponding analytical models predict diffusion-like macroscale response and provide explicit expressions for the effective diffusion coefficients in terms of the microstructure of the porous medium and flow conditions. A parallel experimental study is conducted to corroborate analytical predictions. Results confirm the relevance of pore-scale mixing in cyclic flow as a transport mechanism in porous networks.

Keywords Porous media · Solute · Transport · Dispersion

1 Introduction

Cyclic flow with zero time-average velocity takes place in porous networks subjected to periodic excitation. Potential examples include the cyclic flow in bones prompted by physical exercise, cyclic flow of contaminants in soils subjected to dynamic loads and saltwater intrusion into fresh water reservoirs due to tidal action. The geometry of the porous network and non-uniform flow conditions cause a relatively high rate of mixing within pores. As a result, even though the effective advection is null in cyclic flow, solute is transported at a much faster rate than possible by diffusion alone in the absence of fluid flow.

The relevance of this mechanism for nutrient transport in bones was first suggested by Wang et al. (2000). They studied an ideal 1D porous network by means of numerical computations. For more discussions on the role of fluid flow in the transport of nutrients in bones see

J. J. Claria · G. H. Goldsztein (✉) · J. C. Santamarina
Georgia Institute of Technology, Atlanta, GA, USA
e-mail: ggold@math.gatech.edu

Piekarski and Munro (1977), Cedergren (1989), Dagan (1989), Bear and Bachmat (1990), Gelhar et al. (1992), Brusseau (1994), Feyen et al. (1998), Vogel and Chrysikopoulos (2002), Cirpa and Attinger (2003), Knothe Tate and Knothe (2000), Knothe Tate (2001). Other studies of transport processes in porous media can be found in Saffman (1959a,b, 1960), Mei (1992), Brenner and Edwards (1993), and Hornung (1997). In particular, we note that the transport process described herein fundamentally differs from the Taylor–Aris dispersion (Taylor 1953; Aris 1956, 1959) and cannot be explained by Aris' pulsating flow model (Aris 1960).

The purpose of this article is to present theoretical solutions of this transport mechanism for two types of porous networks and boundary conditions, followed by an experimental validation. We obtain explicit formulae for the effective diffusion coefficients in terms of the geometry of the medium and the flow conditions. As the time-average flow velocity is zero and the networks exhibit a macroscopic diffusion-like behavior, we call this transport mechanism "AC diffusion".

2 Mathematical Model

Our two ideal porous networks are displayed in Fig. 1. They consist of large pores or lacunae interconnected by thin channels. In both networks, the first channel is connected to a reservoir of solute at the origin of the coordinate system, $x = 0$. The location of the ith channel is the segment $[(i-1)L, iL-l]$ and the location of ith pore is $[iL-l, iL]$. The cross-sectional area of a channel is a. We denote by $V_c = (L-l)a$ and V_l the volume of each channel and pore, respectively. The network in Fig. 1a extends to infinity and is rigid, i.e., V_c and V_l are constants independent of time. On the other hand, the network of Fig. 1b contains a finite number N of compressible lacunae of equal volume V_l that is assumed to be a known periodic function of time t with period t_0. The channels are assumed of constant volume.

An incompressible fluid with uniform density fills the networks. The solute concentration in the reservoir remains at the constant value c_0, while the solute concentration is initially 0 elsewhere.

We assume 1D flow within the channels. Thus, fluid incompressibility and mass conservation imply that the fluid velocity in the channel v is independent of x

$$v(x,t) = v_i(t) \text{ if } x \in i\text{th channel}. \tag{1}$$

Conservation of mass in the ith pore implies

$$\frac{dV_l}{dt} = a(v_i - v_{i+1}), \tag{2}$$

where we take $v_{N+1} = 0$ for the compressible system.

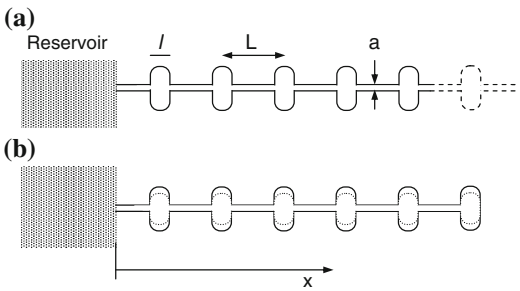

Fig. 1 Idealized 1D networks. **a** Rigid network with cyclic flow through. **b** Compressible network subjected to cyclic compression with only one open boundary

Note that a consequence of Eq. 2 is that the fluid velocities in all channels are equal in the rigid system. This velocity is denoted by $v(t)$ and is assumed to be a known periodic function of t with period t_0, i.e.,

$$v_i(t) = v(t) \text{ for the rigid network.} \tag{3}$$

On the other hand, Eq. 2 implies

$$v_i(t) = \frac{N-i+1}{a}\frac{\mathrm{d}V_1}{\mathrm{d}t} \text{ for the compressible network.} \tag{4}$$

We assume that mixing within each pore occurs in time scales much shorter than t_0 so that we can assume that mixing is instantaneous within each pore. We denote by $c_i(t)$ the concentration of nutrients at time t in the ith pore.

For x in the channels, we denote by $c(x,t)$ the concentration of nutrients at x and time t. We neglect mixing within the channels (to highlight the difference with Taylor–Aris dispersion). Thus, the solute flows with the same velocity as the fluid within the channels and the equation for solute conservation within the channels reduces to

$$\frac{\partial c}{\partial t} + v_i\frac{\partial c}{\partial x} = 0 \text{ if } x \in i\text{th channel.} \tag{5}$$

Whenever the fluid velocity in a channel is positive, solute flows from the ith channel into the ith pore at a rate $av_i(t)c(iL-l,t)$. Solute also flows out of that same pore into the $(i+1)$th channel at a rate $av_{i+1}(t)c_i(t)$. Analogously, when the velocity is negative, solute flows from the $(i+1)$th channel into the ith lacuna at a rate $-av_{i+1}(t)c(iL,t)$ and flows out of that same pore into the ith channel at a rate $-av_i(t)c_i(t)$. Thus,

$$\frac{1}{a}\frac{\mathrm{d}(V_1c_i)}{\mathrm{d}t} = \begin{cases} v_i(t)c(iL-l,t) - v_{i+1}(t)c_i(t) & \text{when} \quad v_i(t) > 0 \\ v_i(t)c_i(t) - v_{i+1}(t)c(iL,t) & \text{when} \quad v_i(t) < 0. \end{cases} \tag{6}$$

Whenever the velocity is positive, solute flows from the $(i-1)$th pore into the ith channel and thus, the solute concentration in the left-end of ith channel is equal to the solute concentration in the $(i-1)th$ pore. Analogously, whenever the velocity is negative, the solute concentration in the right end of ith channel is equal to the solute concentration in the ith pore. Mathematically,

$$\begin{aligned} c((i-1)L,t) &= c_{i-1}(t) \quad \text{if} \quad v_i(t) > 0 \\ c(iL-l,t) &= c_i(t) \quad \text{if} \quad v_i(t) < 0. \end{aligned} \tag{7}$$

Note that the above equation is also valid for $i = 1$ taking $c_0(t) = c_0$, the concentration of solute in the reservoir.

The initial concentration in the network is 0, thus

$$c_i(0) = 0 \quad i > 0. \tag{8}$$

We assume that the flow velocity in the channels v has zero time average, in both rigid and compressible cases,

$$\int_0^{t_0} v(t)\mathrm{d}t = 0. \tag{9}$$

In the rigid case, we assume that there exist $0 < t^* < t_0$ such that $v(t) > 0$ if $0 < t < t^*$ and $v(t) < 0$ if $t^* < t < t_0$. Thus, the volume of fluid that flows from the reservoir into the network in the time interval $0 < t < t^*$ is

$$V_{\mathrm{F}} = a \int_0^{t^*} v(t)\mathrm{d}t. \tag{10}$$

Our analysis shows that the effective diffusion of the rigid system is D_{r}, defined in Eq. 19. More precisely, let $\rho = \rho(z, t)$ be the solution of

$$\frac{\partial \rho}{\partial t} = D_{\mathrm{r}} \frac{\partial^2 \rho}{\partial z^2} \quad \text{for} \quad t > 0 \quad \text{and} \quad z > 0, \tag{11}$$

subjected to the initial conditions

$$\rho(z, 0) = 0 \quad \text{for} \quad z > 0 \tag{12}$$

and boundary conditions

$$\rho(0, t) = c_0 \quad \text{and} \quad \lim_{z \to +\infty} \rho(z, t) = 0 \quad \text{for} \quad t \geq 0. \tag{13}$$

Extend the definition of ρ to $z < 0$ as follows:

$$\rho(z, t) = c_0 \quad \text{if} \quad z \leq 0, \tag{14}$$

and let $z_i = z_i(t)$ be defined as

$$z_i(t) = iL - \frac{aL}{V_{\mathrm{l}} + V_{\mathrm{c}}} \int_0^t v(s)\mathrm{d}s. \tag{15}$$

Note that the variable z is like a Lagrangian coordinate, which is related to the original space variable x by the formula

$$z = x - \frac{aL}{V_{\mathrm{l}} + V_{\mathrm{c}}} \int_0^t v(s)\mathrm{d}s. \tag{16}$$

We show that ρ gives the asymptotic approximation of the concentrations, i.e.,

$$c_i(t) \cong \rho(z_i(t), t) \text{ if } V_{\mathrm{F}} \gg V_{\mathrm{c}}. \tag{17}$$

This system of equations can be solved explicitly,

$$\rho(z, t) = c_0 - c_0 \int_0^{z/(2\sqrt{D_{\mathrm{r}}t})} \exp(-s^2)\mathrm{d}s. \tag{18}$$

Our analysis shows that the effective diffusion coefficient D_{r} is (Goldsztein and Santamarina 2004)

$$D_{\mathrm{r}} = \left(\frac{V_{\mathrm{l}}}{V_{\mathrm{c}} + V_{\mathrm{l}}}\right)^2 \left(\frac{V_{\mathrm{F}}}{V_{\mathrm{c}} + V_{\mathrm{l}}}\right) \left(\frac{L^2}{t_0}\right). \tag{19}$$

Note D_{r} is determined by the periodicity t_0 and the invaded volume V_{F}, and is unaffected by other characteristics of the function selected for the fluid velocity in channels.

In the compressible case, we assume that there exist $0 < t^* < t_0$ such that the volume of each lacuna $V_l(t)$ increases in the time interval $0 < t < t^*$ and decreases in the time interval $t^* < t < t_0$. Thus, the difference between the largest and smallest value $V_l(t)$ is

$$\Delta V_l = \frac{1}{2} \int_0^{t_0} \left| \frac{\mathrm{d}V_l}{\mathrm{d}t}(t) \right| \mathrm{d}t. \tag{20}$$

We denote the average of $V_l(t)$ by $\langle V_l \rangle$

$$\langle V_l \rangle = \frac{1}{t_0} \int_0^{t_0} V_l(t) \mathrm{d}t. \tag{21}$$

Let

$$D_\mathrm{f} = N \left(\frac{\Delta V_l}{\langle V_l \rangle} \right) \left(\frac{L^2}{t_0} \right) \tag{22}$$

and $\rho = \rho(x, t)$ be the solution

$$\frac{\partial \rho}{\partial t} = D_\mathrm{f} \frac{\partial}{\partial x} \left(\left(1 - \frac{x}{NL} \right) \frac{\partial \rho}{\partial x} \right) \quad \text{for} \quad t > 0 \quad \text{and} \quad 0 \le x \le NL \tag{23}$$

subjected to the initial conditions

$$\rho(x, 0) = 0 \quad \text{for} \quad 0 \le x \le NL, \tag{24}$$

and boundary conditions

$$\rho(0, t) = c_0 \quad \text{and} \quad \frac{\partial \rho}{\partial x}(NL, t) = 0 \quad \text{for} \quad t > 0. \tag{25}$$

We show that ρ gives the asymptotic approximation of the concentrations, more precisely, if

$$\frac{V_\mathrm{c}}{\langle V_l \rangle} \ll 1, \quad \frac{\Delta V_l}{\langle V_l \rangle} \ll 1, \quad N \gg 1 \quad \text{and} \quad \frac{V_\mathrm{c}}{\Delta V_l} \ll 1, \tag{26}$$

then

$$c_i(t) \cong \rho(iL, t). \tag{27}$$

The value $D_\mathrm{f}(1 - x/(NL))$ in Eq. 23 is the effective diffusion coefficient. Note that the diffusion coefficient varies in space, decreasing linearly from D_f at the open boundary to zero at the closed boundary, analogous to the decreasing cyclic flow. Therefore, AC diffusion vanishes toward the closed boundary. The derivation equations (22–27) are given in the Appendix.

3 Experimental Study

Experiments were designed to study AC diffusion in compressible and rigid network systems and the associated boundary conditions.

The case of a rigid network with cyclic flow through was investigated with a packing of glass beads (1.5-mm diameter, packing porosity $n \approx 0.33$), held within a flexible latex membrane in the shape of a cylindrical specimen (60-mm tall and 25-mm diameter). A pressure of 90 kPa is hydraulically applied onto the membrane to render the granular skeleton rigid.

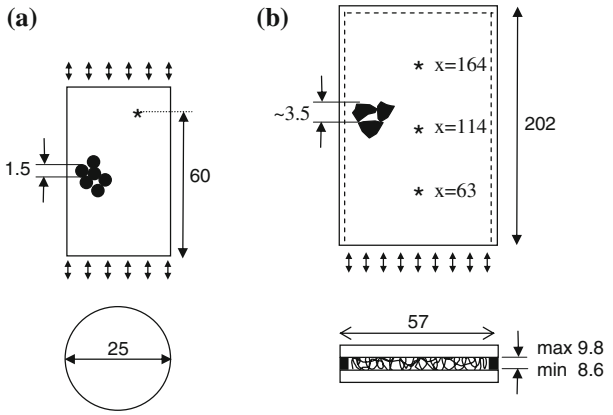

Fig. 2 Physical models—experimental study. **a** Rigid network with cyclic flow through. **b** Compressible network subjected to cyclic compression with only one open boundary. Note: sketches not to scale; *asterisks* denote measurement points; all dimensions in millimeter

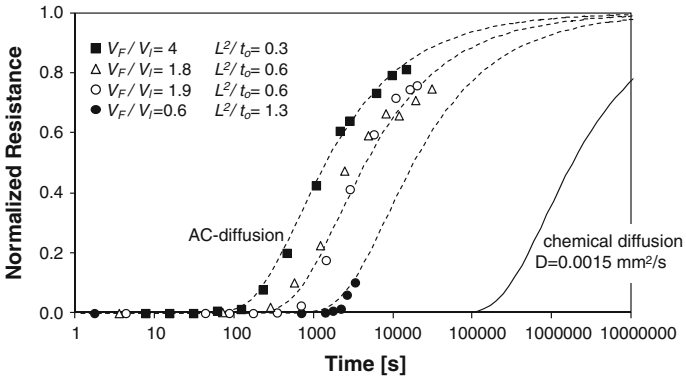

Fig. 3 Rigid network with cyclic flow through. Entry and exit boundaries remain open. High concentration is maintained in the lower boundary. Data points are experimental results (Note: there are four separate tests). Analytical predictions are shown as *dashed lines* for various diffusion coefficients (refer to Table 1)

Cyclic flow is imposed through the lower end using a syringe pump, while free drainage conditions are allowed at the upper end. The porous medium is filled with deionized water, while the pore fluid cycled trough the lower boundary is a 0.3 M NaCl solution. The arrival of the diffusion front at $x = 60$ mm is detected with a 1.5-mm diameter electrical conductivity probe placed near the upper cap (schematic and details in Fig. 2a).

Various tests were conducted by imposing cyclic volumes that ranged between $V_F/V_l = 60$ and 400 and cyclic frequencies between 0.1 and 0.6 Hz. The frequency–volume combinations were selected to render similar peak flow rates (1.1–1.6 cm^3/s). Results for four tests are presented in Fig. 3 in terms of normalized concentration versus time (Note: the diffusion fronts arrive around cycles ~20 and ~1, 200 for the highest and lowest cyclic volumes, respectively). The theoretical solution to the diffusion equation is fitted to invert the effective AC-diffusion coefficient D (Eqs. 11, 19).

The case of a compressible network with only one open boundary was studied with a packing of rubber particles (diameter 3.5 mm) held between two parallel rigid plates with closed

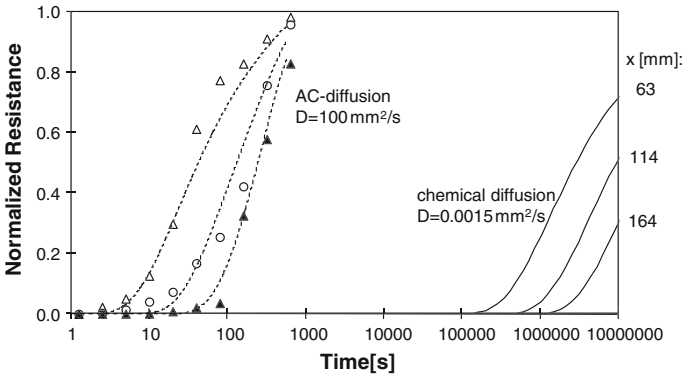

Fig. 4 Compressible network subjected to cyclic compression with only one open boundary; high ionic concentration is maintained outside this boundary. Data points are experimental results (Note: measurements at distance $x = 63$, 114, and 164 mm). Analytical predictions shown as *dotted lines* correspond to Eq. 23. Trends for chemical diffusion on the *right* are predicted for standard diffusion under hydrostatic conditions at different x-locations

fluid flow on three sides, forming a specimen 202-mm long and 57-mm wide. The plates were cyclically compressed against each other (frequency 0.8 Hz; cyclic volume change relative to pore volume $\Delta V_l / V_l = 60 \approx 0.12$). The evolution of the concentration front was monitored with three electrical probes mounted through the top plate as shown in Fig. 2b. Data gathered in three separate tests are presented in Fig. 4. The theoretical solution (Eq. 23) is simultaneously adjusted to the three measurement sets by fitting only one parameter D_f.

4 Discussion and Conclusions

Clearly, experiments involve a more complex pore topology than that assumed in the analyses. Yet, in both experiments and analyses, the global flow is 1D (i.e., x-direction in model channels) while mixing presumes multi-directional fluid motion in pores (i.e., lacunae in the model).

The AC-diffusion coefficients are predicted using pore-scale parameters estimated for the two tested systems (Eqs. 19, 22) and inverted by matching the experimental measurements (Eqs. 11 and 23—Note: the inter-pore distance L is assumed to scale with the grain size). Predicted and fitted coefficients are compared in Table 1. For clarity, the concentration-time trends for chemical diffusion under hydrostatic conditions predicted with a diffusion coefficient for NaCl of $D = 0.0015\,\mathrm{mm}^2/\mathrm{s}$ (infinite medium) are superimposed in Figs. 3 and 4.

There are two important observations. First, the AC-diffusion coefficients predicted using the 1D pore-scale models solved here are in the same order of magnitude as the fitted diffusion values (Table 1). Second, transport by AC diffusion can be orders of magnitude more efficient than diffusive transport in a hydrostatic system; for example, the validation experiments show 10^2 to 10^5 shorter times (see analytical predictions and experimental results in Table 1; Figs. 3, 4). Therefore, both analytical and experimental results confirm the relevance of pore-scale mixing in chemical transport when porous networks are subjected to cyclic fluid flow.

The AC-diffusion coefficients are macroscopic parameters, i.e., the length scale of the phenomenon is much larger than the pore scale. Yet, they do involve the internal length scale

Table 1 Comparison between predicted diffusion coefficients (based on microscale properties) and fitted values

System	Predicted AC diffusion (based on pore-scale information)				Diffusion coefficient D fitted to the data (mm^2/s)
	Equation	Parameters		D predicted from microstructure (mm^2/s)	
		$\frac{V_F}{V_l}$	$\frac{L^2}{t_0}$ (mm^2/s)		
Rigid network with cyclic flow through	$D \cong \frac{V_F}{V_l}\frac{L^2}{t_0}$	0.6	1.3	0.8	0.15
		1.8	0.6	1.1	0.6
		4	0.3	1.2	1.9
Compressible network with one open boundary, under cyclic compression	$D \cong \frac{\Delta V_l}{V_l}\frac{NL^2}{t_0}$	$\frac{\Delta V_l}{V_l} \sim 0.12$	$N \sim 60$ $\frac{L^2}{t_0} \sim 10$	72	100
Chemical diffusion coefficient (in bulk fluid)				0.001–0.003 mm^2/s	

of the porous medium through the pore volume and the pore-to-pore distance. The analytical solution for the effective AD diffusion coefficients reveals the interplay between the physical parameters involved.

Acknowledgments Support for this research was provided by the Goizueta Foundation and the National Science Foundation.

Appendix

We define the function $f = f(s)$ as follows

$$V_l = \langle V_l \rangle \, (1 + \delta f \, (t/t_0)) \tag{28}$$

where

$$\int_0^1 |f'(s)| \mathrm{d}s = 1, \tag{29}$$

where f' is the derivative of f. Note that f is periodic, with period one and zero average. We also define

$$a_i = 1 - \frac{(i-1)}{N} \tag{30}$$

and

$$\varepsilon = \frac{V_c}{\langle V_l \rangle \, \delta N}, \tag{31}$$

which we assume small

$$\varepsilon \ll 1. \tag{32}$$

Simple calculations show that

$$v_i(t) = \frac{a_i}{\varepsilon}\frac{(L-l)}{t_0} f'(t/t_0). \tag{33}$$

We define

$$\beta_i = \begin{cases} \varepsilon t_0 \left(\frac{1}{a_i f'(t/t_0)} + \varepsilon \frac{f''(t/t_0)}{2a_i^2 (f'(t/t_0))^3} \right) & \text{if} \quad f'(t/t_0) > 0 \\ \varepsilon t_0 \left(-\frac{1}{a_{i+1} f'(t/t_0)} + \varepsilon \frac{f''(t/t_0)}{2a_{i+1}^2 (f'(t/t_0))^3} \right) & \text{if} \quad f'(t/t_0) < 0. \end{cases} \tag{34}$$

In Sect. A.1 below we show that

$$\begin{aligned} c\left(iL - l, t\right) &\approx c_{i-1}\left(t - \beta_i\right) \quad \text{if} \quad f'(t/t_0) > 0 \\ c\left(iL, t\right) &\approx c_{i+1}\left(t - \beta_i\right) \quad \text{if} \quad f'(t/t_0) < 0. \end{aligned} \tag{35}$$

We use this last equation to transform Eq. 6 in

$$\frac{1}{a}\frac{\mathrm{d}\left(V_l c_i\right)}{\mathrm{d}t} = \begin{cases} v_i(t) c_{i-1}(t - \beta_i) - v_{i+1}(t) c_i(t) & \text{if} \quad f'(t/t_0) > 0 \\ v_i(t) c_i(t) - v_{i+1}(t) c_{i+1}(t - \beta_i) & \text{if} \quad f'(t/t_0) < 0. \end{cases} \tag{36}$$

We propose the anzats

$$c_i(t) = \rho\left(y = i/N, \tau = t/t_0\right). \tag{37}$$

We set

$$\alpha_1 = \frac{1}{\varepsilon N}, \quad \alpha_2 = \frac{\delta}{\varepsilon} \tag{38}$$

assume that both α_1 and α_2 to be order 1 quantities, and define

$$b(x, \tau) = \begin{cases} \varepsilon \frac{1}{(1-x+\alpha_1\varepsilon) f'} + \varepsilon^2 \frac{f''}{2(1-x+\alpha_1\varepsilon)^2 (f')^3} & \text{if} \quad f' > 0 \\ -\varepsilon \frac{1}{(1-x) f'} + \varepsilon^2 \frac{f''}{2(1-x)^2 (f')^3} & \text{if} \quad f' < 0, \end{cases} \tag{39}$$

where f' and f'' are evaluated at τ. Plugging the above anzats (37) into Eq. 36, making use of the above equations, and simple manipulations lead to

$$\begin{aligned} &\frac{\alpha_1}{\alpha_2}\frac{\partial\left[\left(1 + \alpha_2 \varepsilon f\right)\rho(x, \tau)\right]}{\partial \tau} \\ &= \begin{cases} \left(1 - x + \alpha_1\varepsilon\right) f' \rho\left(x - \alpha_1\varepsilon, \tau - b\right) - (1 - x) f' \rho(x, \tau) & \text{if} \quad f' > 0 \\ \left(1 - x + \alpha_1\varepsilon\right) f' \rho(x, \tau) - (1 - x) f' \rho\left(x + \alpha_1\varepsilon, \tau - b\right) & \text{if} \quad f' < 0 \end{cases} \end{aligned} \tag{40}$$

where f and f' are evaluated at τ, b is evaluated at (x, τ).

We now follow standard two-time scale asymptotic techniques. We introduce a slow time variable

$$\theta = \varepsilon^2 \tau, \tag{41}$$

propose the anzats

$$\rho = \rho_0(x, \theta) + \varepsilon \rho_1(x, \tau) + \varepsilon^2 \rho_2(x, \tau). \tag{42}$$

Plug this anzats into Eq. 40. Expand in powers of ε to get at $O(\varepsilon)$

$$\frac{\alpha_1}{\alpha_2}\frac{\partial \rho_1}{\partial \tau} = -\alpha_2 f' \rho_0 - \alpha_1 f' \frac{\partial\left((1-x)\rho_0\right)}{\partial x} \tag{43}$$

and at $O(\varepsilon^2)$

$$\frac{\alpha_1}{\alpha_2}\left(\frac{\partial \rho_2}{\partial \tau} + \frac{\partial \rho_0}{\partial \theta}\right) + (1+\alpha_1 f)\frac{\partial \rho_1}{\partial \tau} = (1-x)\left(\frac{|f'|}{2}\alpha_1^2 \frac{\partial^2 \rho_0}{\partial x^2} - f'\alpha_1 \frac{\partial \rho_1}{\partial x}\right) - f'_+ \alpha_1^2 \frac{\partial \rho_0}{\partial x}, \tag{44}$$

where $f'_+ = \max\left\{f', 0\right\}$. From Eq. 43 we obtain ρ_1,

$$\frac{\alpha_1}{\alpha_2}\rho_1 = -\alpha_2 f \rho_0 - \alpha_1 f \frac{\partial\left((1-x)\rho_0\right)}{\partial x}. \tag{45}$$

We now require ρ_2 to be periodic in τ with period 1, replace the expression for ρ_1 (Eq. 45) into Eq. 44, integrate the result over one period in τ to get

$$\frac{\partial \rho_0}{\partial \theta} = \frac{\alpha_1 \alpha_2}{2}\left(\int_0^1 |f'(s)|\mathrm{d}s\right)\frac{\partial\left((1-x)\frac{\partial \rho_0}{\partial x}\right)}{\partial x}, \tag{46}$$

which, after going back to the dimensional variables, reduces to Eq. 23.

A.1 Derivation of Eqs. 34–35

Let $X = X(s)$ be a solution of

$$X'(s) = v_i(s) \quad \text{and } X(t) = iL - l. \tag{47}$$

Fix t and let $\beta_i > 0$. If $(i-1)L \le X(s) \le iL - l$ for all $s \in [t-\beta_i, t]$, then, Eq. 5 implies that c is constant along the characteristic paths, and thus, $c\left(X(s), s\right)$ is independent of s for $s \in [t-\beta_i, t]$. Thus, assuming that $v_i(s) > 0$ for all $s \in [t-\beta_i, t]$ and β_i is implicitly given by the equation

$$X(t-\beta_i) = (i-1)L, \tag{48}$$

we have that $c\left(iL-l, t\right) = c\left(X(t), t\right) = c\left(X(t-\beta_i), t-\beta_i\right) = c\left((i-1)L, t-\beta_i\right)$. On the other hand, as $v_i(t-\beta_i) > 0$, Eq. 7 implies that $c\left((i-1)L, t-\beta_i\right) = c_{i-1}(t-\beta_i)$. Thus,

$$c\left(iL-l, t\right) = c_{i-1}(t-\beta_i). \tag{49}$$

We now proceed to compute β_i. Using Taylor expansions, we have $X(t') \approx X(t) + v_i(t)(t'-t) + v'(t)(t'-t)^2/2$ for $|t'-t| \ll t_0$. Thus, using Eq. 33 we obtain

$$X(t') \approx X(t) + \frac{a_i}{\varepsilon}\frac{(L-l)}{t_0} f'(t/t_0)(t'-t) + \frac{1}{2}\frac{a_i}{\varepsilon}\frac{(L-l)}{t_0^2} f''(t/t_0)(t'-t)^2 \quad \text{for} \quad |t'-t| \ll t_0. \tag{50}$$

Using this approximation in Eq. 48 we get

$$(i-1)L \approx iL - 1 - \frac{a_i}{\varepsilon}\frac{(L-l)}{t_0} f'(t/t_0)\beta_i + \frac{1}{2}\frac{a_i}{\varepsilon}\frac{(L-l)}{t_0^2} f''(t/t_0)\beta_i^2. \tag{51}$$

We substract $(i-1)L$ on both sides of the above equation, then multiply by $\varepsilon/(L-l)$ to get

$$0 \approx \varepsilon - a_i f'(t/t_0)\frac{\beta_i}{t_0} + \frac{1}{2}a_i f''(t/t_0)\frac{\beta_i^2}{t_0^2}. \tag{52}$$

From Eq. 52, expanding β_i in powers of ε and noting that $v_i(t)$ and $f'(t/t_0)$ have the same sign, it is easy to show that Eqs. 34 and 35 are valid for $f'(t/t_0) > 0$. Similar arguments show that those equations are also valid when $f'(t/t_0) < 0$.

References

Aris, R.: On the dispersion of a solute in a fluid flowing through a tube. Proc. R. Soc. Lond. A **235**, 67–77 (1956)

Aris, R.: On the dispersion of a solute by diffusion, convection, and exchange between phases. Proc. R. Soc. Lond. A **252**, 538–550 (1959)

Aris, R.: On the dispersion of a solute in pulsating flow through a tube. Proc. R. Soc. Lond. A **259**, 370–376 (1960)

Bear, J., Bachmat, Y.: Introduction to Modeling of Transport Phenomena in Porous Media. Kluwer Academic Publishers, Boston (1990)

Brenner, H., Edwards, D.A.: Macrotransport Processes. Butterworth-Heinemann Series in Chemical Engineering, Stoneham, MA (1993)

Brusseau, M.L.: Transport of reactive contaminants in heterogeneous porous media. Rev. Geophys. **32**, 285–313 (1994)

Cedergren, H.R.: Seepage, Drainage, and Flow Nets. Wiley, Seattle, WA (1989)

Cirpa, O.A., Attinger, S.: Effective dispersion in heterogeneous media under random transient flow conditions. Water Resour. Res. **39**, 1–15 (2003)

Dagan, G.: Flow and Transport in Porous Formations. Springer, New York (1989)

Feyen, J., Jacques, D., Timmerman, A., Vanderborght, J.: Modeling water flow and solute transport in heterogeneous soils: a review of recent approaches. J. Agric. Engng. Res. **70**, 231–256 (1998)

Gelhar, L.W., Welty, C., Rehfeldt, K.R.: A critical review of data on field-scale dispersion in aquifers. Water Resour. Res. **28**, 1955–1974 (1992)

Goldsztein, G.H., Santamarina, J.C.: Solute transport during cyclic flow in saturated porous media. Appl. Phys. Lett. **85**, 2432–2434 (2004)

Hornung, U: Miscible displacement. In: Hornung, U. (ed.) Homogenization and Porous Media, Springer, New York (1997)

Knothe Tate, M.L.: Mixing mechanisms and net solute transport in bone. Ann. Biomed. Eng. **29**, 810–811 (2001)

Knothe Tate, M.L., Knothe, U.: An ex vivo model to study the transport processes and fluid flow in loaded bone. J. Biomech. **33**, 247–254 (2000)

Mei, C.C.: Method of homogenization applied to dispersion in porous media. Transp. Porous Media **9**, 261–274 (1992)

Piekarski, K., Munro, M.: Transport mechanism operating between blood supply and osteocytes in long bones. Nature **269**, 80–82 (1977)

Saffman, P.G.: A theory of dispersion in a porous medium. J. Fluid Mech. **6**, 321–349 (1959a)

Saffman, P.G.: Dispersion flow trough a network of capillaries. Chem. Eng. Sci. **11**, 125–129 (1959b)

Saffman, P.G.: Dispersion due to molecular diffusion and macroscopic mixing in flow trough a network of capillaries. J. Fluid Mech. **7**, 194–208 (1960)

Taylor, G.: The instability of liquid surfaces when accelerated in a direction perpendicular to their planes. Proc. R. Soc. Lond. A **201**, 192–196 (1953)

Vogel, E.T., Chrysikopoulos, C.V.: Experimental investigation of acoustically enhanced solute transport in porous media. Geophys. Res. Lett. **29**, 1–4 (2002)

Wang, L., Cowin, S.C., Weinbaum, S., Fritton, S.P.: Modeling tracer transport in an osteon under cyclic loading. Ann. Biomed. Eng. **28**, 1200–1209 (2000)